ARTICLES

Gas Phase Study of the Clustering Reactions of $C_2H_5^+$, *s*-$C_3H_7^+$, and *t*-$C_4H_9^+$ with CO_2 and N_2O: Isomeric Structure of $C_2H_5^+$, $C_2H_5^+(CO_2)_n$, and $C_2H_5^+(N_2O)_n$

Kenzo Hiraoka,* Takashi Shoda, Ichiro Kudaka, Susumu Fujimaki, and Susumu Mizuse

Clean Energy Research Center, Yamanashi University, Takeda-4, Kofu 400-8511, Japan

Shinichi Yamabe*

Department of Chemistry, Nara University of Education, Takabatake-cho, Nara 630-8528, Japan

Hiroaki Wasada

Faculty of Regional Studies, Gifu University, Yanagido 1-1, Gifu 501-1193, Japan

Yuko Wasada-Tsutsui

Institute of Natural Sciences, Nagoya City University, Nagoya 467-8501, Japan

Received: June 28, 2002; In Final Form: November 19, 2002

The thermochemical stabilities of gas phase cluster ions $C_2H_5^+(Sol)_n$, *s*-$C_3H_7^+(Sol)_n$, and *t*-$C_4H_9^+(Sol)_n$ (Sol = CO_2 and N_2O) were determined using a pulsed electron beam high-pressure mass spectrometer. The stabilities and structures of those cluster ions were studied theoretically by density functional theory calculations. For the free $C_2H_5^+$ ion, not the classical but the nonclassical bridged form is likely to be the major component. B3LYP/6-311+G(2d,p) calculations showed that the classical structure is absent. In the clustering reaction of $C_2H_5^+$ with Sol, a hydrogen bond type loose complex of the nonclassical $C_2H_5^+$ with Sol is initially formed, which is followed by the intramolecular isomerization of $C_2H_5^+$ to the classical structure forming the stronger bond with Sol. Surprisingly small bond energies of 4−5 kcal/mol for *s*-$C_3H_7^+\cdots$Sol and *t*-$C_4H_9^+\cdots$Sol arise from the hyperconjugation effect of methyl groups.

1. Introduction

Investigations on the bonding of cluster ions provide information on the well depth and forces between ions and neutral molecules and the structures of ions and their clusters with neutral molecules.[1−3] Theoretical investigation of the ethyl cation[4] led to the prediction that the classical structure was several kcal/mol more stable than the nonclassical (bridged) structure in Scheme 1.

However, calculations including polarization functions and electron correlation[5] have lowered the stability of the bridged $C_2H_5^+$ to 6.3 kcal/mol below the classical cation. Ausloos et al.[6] observed randomization of H and D in partially deuterated ethyl cations by the methods of kinetic mass spectrometry and chemical end product analysis, suggesting rapid H/D scrambling. From a photoelectron spectroscopy study of C_2H_5, Houle and Beauchamp[7] suggested that the bridged ion is about 3 kcal/mol more stable than the classical one. Porter and co-workers[8] studied the structures of the ethyl radical and cation by neutralized ion beam spectroscopy. They estimated that the bridged structure is 0.8 kcal/mol more stable than the classical one. Hirao and Yamabe[9] made a computational determination of the stabilities of classical and bridged $C_2H_5^+$. According to their results, the bridged form is 4.1 kcal/mol more stable than the classical one. As described above, the bridged $C_2H_5^+$ is predicted to be more stable than the classical one. Rigorously speaking, however, it has not been fully clarified whether the classical structure is in the bound state (local energy minimum) or is only in an intermediate state.

SCHEME 1: Isomeric Structures of Ethyl Cation, $C_2H_5^+$

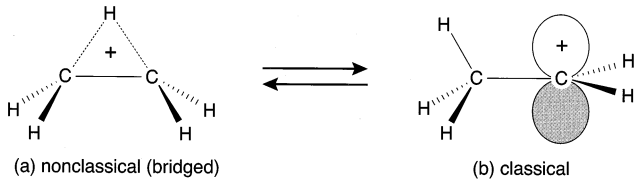

Hiraoka and Kebarle[10] studied the clustering reaction of $C_2H_5^+$ with H_2. At the lowest temperature range, they found that the reaction was the normal clustering reaction with the rate of negative temperature dependence. At higher temperatures, the temperature dependence became positive, suggesting that the reaction was endothermic. Analyzing these temperature dependences, they concluded that the bridged structure of $C_2H_7^+$ (i.e., C−C protonated ethane) is more stable than the classical $C_2H_5^+\cdots H_2$ by 7.8 kcal/mol. Lee et al.[11] measured the infrared spectra of the pentacoordinated $C_2H_7^+$ using a tandem mass spectrometer with a radio frequency octapole ion trap. The

10.1021/jp0215264 CCC: $25.00
Published on Web 01/21/2003

infrared spectra obtained can be attributed to the presence of the classical and bridged protonated ethane.

In the present work, the gas phase equilibria for clustering reactions 1−3 (Sol = CO_2 and N_2O as bases) were studied using a pulsed electron beam high-pressure mass spectrometer.

$$C_2H_5^+(Sol)_{n-1} + Sol = C_2H_5^+(Sol)_n \quad (1)$$

$$s\text{-}C_3H_7^+(Sol)_{n-1} + Sol = s\text{-}C_3H_7^+(Sol)_n \quad (2)$$

$$t\text{-}C_4H_9^+(Sol)_{n-1} + Sol = t\text{-}C_4H_9^+(Sol)_n \quad (3)$$

The main objective of the present work is to obtain the thermochemical data for these reactions and the structural information on the cluster ions of the three carbonium ions with isoelectronic CO_2 and N_2O molecules.[12] A systematic study of the solvent strength of these ions may provide intrinsic information about the stability of carbonium ions, which are important intermediates in S_N1 reactions.

2. Experimental and Computational Methods

The measurements were made with a pulsed electron beam high-pressure mass spectrometer, which has been described previously.[13] Briefly, the sample gas at 2−4 Torr was ionized by a pulsed 2 keV electron beam. The ions produced were sampled through a slit made of razor blades (1 mm × 0.015 mm). The ions escaping from the field free ion source into an evacuated region were analyzed by a quadrupole mass spectrometer (ULVAC, MSQ-400, m/z = 1−550) and collected in a multichannel analyzer as a function of their arrival time after the electron pulse.

$C_2H_5^+(Sol)_n$ System. The major gas CH_4 (Iwatani, UHP) at 2−4 Torr was purified by passing it through a liquid nitrogen-cooled 5 A molecular sieve trap. CO_2 or N_2O ((10−50) × 10^{-3} Torr) was added into the major CH_4 gas through a stainless steel capillary (1m in length × 0.1 mm in diameter). The $C_2H_5^+$ ions are produced by the reaction of CH_3^+ with CH_4.

$$CH_3^+ + CH_4 = C_2H_5^+ + H_2 \quad (4)$$

Porter and co-workers[8] produced $C_2H_5^+$ by three ion−molecule reactions, $CH_3^+ + CH_4 \rightarrow C_2H_5^+ + H_2$, $H_3^+ + C_2H_4 \rightarrow C_2H_5^+ + H_2$, and $C_2H_5Cl + e^- \rightarrow C_2H_5^+ + Cl + 2e^-$. They found that neutral beam profiles for ethyl radicals formed by the neutralization of $C_2H_5^+$ ions generated by three methods of ionization were exactly the same. This indicates that all of the $C_2H_5^+$ formed by these methods have the same structure.

$s\text{-}C_3H_7^+(Sol)_n$ System. The major gas CH_4, which was passed through the ice-cooled (0 °C) molecular sieve trap, was used as a reagent gas. CO_2 or N_2O ((10−50) × 10^{-3} Torr) was added into the major CH_4 gas through a stainless steel capillary. An electron impact on the reagent CH_4 gas containing trace amounts of higher hydrocarbons (mainly C_2 and C_3) produced abundant $s\text{-}C_3H_7^+$ ions.

$t\text{-}C_4H_9^+(Sol)_n$ System. *iso*-C_4H_{10} (10^{-4} Torr) and CO_2 or N_2O ((10−50) × 10^{-3} Torr) were added into the major CH_4 gas, which was purified by passing it through a liquid nitrogen-cooled molecular sieve trap. The $t\text{-}C_4H_9^+$ ions are formed by reactions 5 and 6.

$$C_2H_5^+ + i\text{-}C_4H_{10} = t\text{-}C_4H_9^+ + C_2H_6 \quad (5)$$

$$CH_5^+ + i\text{-}C_4H_{10} = t\text{-}C_4H_9^+ + CH_4 + H_2 \quad (6)$$

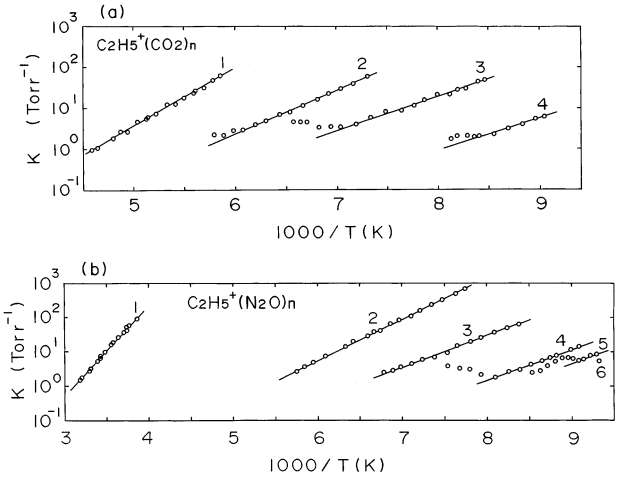

Figure 1. van't Hoff plots for equilibria of the clustering reaction, $C_2H_5^+(Sol)_{n-1} + Sol = C_2H_5^+(Sol)_n$. The deviation of the equilibrium constants with $n \geq 2$ for CO_2 and $n \geq 4$ for N_2O in the higher temperature region is due to the presence of the isomeric cluster ions. Integer numbers stand for n values.

Density functional theory calculations were performed for carbonium ions and their n = 1 and 2 clusters. These geometries were optimized with the B3LYP/6-311+G(2d,p)[14] method. Subsequent vibrational analyses were made to check whether the obtained geometries were at their energy minima. B3LYP/6-311+G(2d,p) zero-point vibrational energies (ZPVEs) were found to be overestimated. Alternatively, RHF/6-311G* ZPVEs were obtained by the use of the established scale factor 0.89. RHF/6-31G* ZPVEs are included in highly accurate calculations such as G2 and G2MP2 and would be applicable to evaluating the binding energies of the present clusters. Thus, those energies are composed of the B3LYP/6-311+G(2d,p) electronic energies and RHF/6-31G* ZPVEs. For $C_2H_5^+$, calculations of B3LYP/6-311+G(3df,2p), MP4(SDQ)/6-311G(d,p), and QCISD(T)/6-311G(d,p) were also performed. All of the calculations were carried out using the GAUSSIAN 94 program[15] installed on the CONVEX C-220 computer (Information Processing Center, Nara University of Education).

3. Experimental Results

3.1. Clustering Reaction of $C_2H_5^+$ with Sol. Figure 1a exhibits the van't Hoff plots for clustering reaction 1 with Sol = CO_2. For n = 1, it takes a few hundred microseconds to establish the equilibria in the higher temperature region due to the slow rate of the forward reaction $C_2H_5^+ + CO_2 \rightarrow C_2H_5^+\text{-}(CO_2)_1$. A loose intermediate complex $[C_2H_5^+\cdots CO_2]^*$ seems to be formed at the initial stage of the formation of the cluster $C_2H_5^+\cdots CO_2$. With decrease of temperature, the rate of the forward reaction becomes increasingly faster and the equilibria with n = 1 could be easily observed. In our previous paper,[16] the nonclassical bridge $C_2H_5^+(a)$ was found to isomerize to the classical $C_2H_5^+(b)$ in the clustering reaction of $C_2H_5^+$ with CH_4. That is, as a free ion, the nonclassical $C_2H_5^+(a)$ is more stable than the classical $C_2H_5^+(b)$[9] while the cluster $C_2H_5^+(b)(CH_4)_n$ is more stable than $C_2H_5^+(a)(CH_4)_n$. The slow establishment of equilibria for reaction 1 with n = 1 also suggests that the more tightly bound $C_2H_5^+(b)\cdots CO_2$ is formed via the loosely bound intermediate $C_2H_5^+(a)\cdots CO_2$.

As shown in Figure 1a, the van't Hoff plots with n = 2−4 deviate from the straight lines at the higher temperature region. In these temperature regions, it was found that the intensities

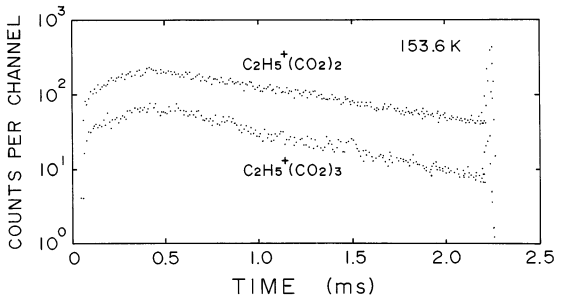

Figure 2. Temporal profiles of $C_2H_5^+(CO_2)_2$ and $C_2H_5^+(CO_2)_3$ ions observed in 2.31 Torr CH_4 and 14 mTorr CO_2. Ion source temperature = 153.6 K, energy of incident electron = 2 keV, electron pulse width = 400 μs. At 2.25 ms, a short positive pulse (25 V) is applied in order to annihilate all ions produced in the ion source. The integration times for the ions $C_2H_5^+(CO_2)_2$ and $C_2H_5^+(CO_2)_3$ are 15 and 150 s, respectively. The faster decay of $C_2H_5^+(CO_2)_3$ than $C_2H_5^+(CO_2)_2$ is due to the isomerization of $C_2H_5^+(a)$ to $C_2H_5^+(b)$.

of the higher clusters $C_2H_5^+(CO_2)_n$ decay faster than those of $C_2H_5^+(CO_2)_{n-1}$ and the equilibria between $C_2H_5^+(CO_2)_n$ and $C_2H_5^+(CO_2)_{n-1}$ could not be observed. The approximate equilibrium constants in Figure 1a were calculated from the ion intensities 2−3 ms after the electron pulse. Figure 2 displays temporal profiles of the $C_2H_5^+(CO_2)_2$ and $C_2H_5^+(CO_2)_3$ ions measured at 153.6 K where approximate "equilibrium constants" deviate from the straight van't Hoff plots. With a decrease of temperature, equilibria could be observed and the equilibrium constants measured at lower temperature region gave straight van't Hoff plots as shown in Figure 1a.

Figure 3a represents the CO_2 pressure dependence on the measured equilibrium constants for reaction 1 with $n = 2-4$. The equilibrium constants with $n = 2$ at 143.5 K and $n = 3$ at 121.5 K are independent of the CO_2 pressure indicating the establishment of the equilibria. In contrast, the values of equilibrium constants with $n = 3$ at 150.5 K and with $n = 4$ at 121.5 K are found to decrease with increase of CO_2 pressure.

The anomaly observed for clustering reaction 1 described above strongly suggests the presence of the isomers for cluster ions. As will be described in Section 4, two stable isomers, $C_2H_5^+(a)(CO_2)_1$ and $C_2H_5^+(b)(CO_2)_1$, are predicted. In the cluster $C_2H_5^+(a)(CO_2)_1$, the thermochemically more stable core ion $C_2H_5^+(a)$ interacts with CO_2. In this case, the interaction between $C_2H_5^+(a)$ and CO_2 is largely electrostatic because the positive charge in the cluster $C_2H_5^+(a)\cdots CO_2$ localizes mainly in the core ion $C_2H_5^+(a)$. In contrast, the semicovalent bond $(CH_3-CH_2-OCO)^+$ is formed in the cluster $C_2H_5^+(b)(CO_2)_1$, and the positive charge is dispersed in the cluster $(CH_3CH_2-OCO)^+$.

The faster decay of $C_2H_5^+(CO_2)_n$ ($n \geq 2$) than $C_2H_5^+(CO_2)_{n-1}$ (see Figure 2) suggests that the initially formed cluster ions $C_2H_5^+(CO_2)_n$ are gradually converted to the smaller cluster ions $C_2H_5^+(CO_2)_{n-1}$. It is likely that the initially formed $C_2H_5^+(a)(CO_2)_n$ isomerizes to more stable $C_2H_5^+(b)(CO_2)_n$ with time. Because the positive charge in the $n = 1$ cluster $[C_2H_5^+(b)\cdots CO_2]$ is more dispersed than that in $C_2H_5^+(a)\cdots CO_2$, the thermochemical stability of $C_2H_5^+(b)(CO_2)_n$ must be lower than that of $C_2H_5^+(a)(CO_2)_n$. This may lead to the conversion of $C_2H_5^+(a)(CO_2)_n$ to $C_2H_5^+(b)(CO_2)_{n-1}$ as is observed in Figure 2.

As shown in Figure 3a, the equilibrium constants for reaction 1 with $n = 3$ at 150.5 K and with $n = 4$ at 121.5 K decrease with increase of CO_2 pressure and asymptotically approach the equilibrium values. This suggests that the isomerization of the core ion $C_2H_5^+(a)$ to $C_2H_5^+(b)$ is enhanced by the presence of

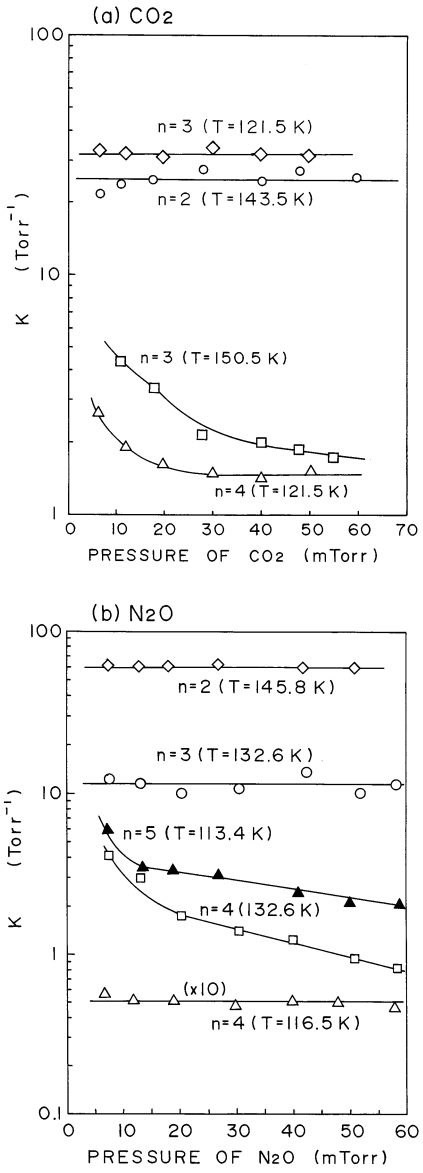

Figure 3. Temperature and Sol pressure dependence on the equilibrium constants for reaction, $C_2H_5^+(Sol)_{n-1} + Sol = C_2H_5^+(Sol)_n$.

CO_2 molecules. Because the isomerization reaction $a \rightarrow b$ is observed down to 121.5 K (Figures 1a and 2), the activation energy for the isomerization reaction seems to be surmountable at these temperatures.

Figure 4a displays the bond dissociation energies ($-\Delta H_{n-1,n}^\circ$) of the cluster ions $C_2H_5^+(CO_2)_n$ vs n. Those energies and entropy changes are listed in Table 1. A rapid decrease of the values $-\Delta H_{n-1,n}^\circ$ with $n = 1 \rightarrow 2$ comes from the fact that an incipient covalent bond is formed in the cluster $C_2H_5^+(b)\cdots CO_2$ (i.e., charge dispersal in the $n = 1$ cluster). The $-\Delta H_{1,2}^\circ$ value is almost the same with that for reaction 2, and the $-\Delta H_{n-1,n}^\circ$ with $n \geq 3$ become smaller than those for reaction 2. This clearly indicates that the positive charge is delocalized in the core ion $(CH_3CH_2-OCO)^+$ and the interactions in the clusters $(CH_3-CH_2-OCO)^+(CO_2)_{n-1}$ become mainly electrostatic.

In clustering reaction 1 with $n = 1$, a greater part of $C_2H_5^+$ must be composed of $C_2H_5^+(a)$ because $C_2H_5^+(a)$ is predicted to be 4.1 kcal/mol more stable than $C_2H_5^+(b)$.[9] On the other hand, the $C_2H_5^+$ in the cluster $C_2H_5^+(CO_2)_1$ has the classical structure b. Thus, the thermochemical data obtained for reaction

TABLE 1: Experimental Thermochemical Data ($-\Delta H_{n-1,n}^\circ$ and $-\Delta S_{n-1,n}^\circ$) for Clustering Reactions, $R^+(Sol)_{n-1} + Sol = R^+(Sol)_n$, $R^+ = C_2H_5^+$, $s = C_3H_7^+$, and $t = C_4H_9^+$, and Sol = CO_2 and N_2O[a]

	$C_2H_5^+$				s-$C_3H_7^+$				t-$C_4H_9^+$			
	$-\Delta H_{n-1,n}^\circ$		$-\Delta S_{n-1,n}^\circ$		$-\Delta H_{n-1,n}^\circ$		$-\Delta S_{n-1,n}^\circ$		$-\Delta H_{n-1,n}^\circ$		$-\Delta S_{n-1,n}^\circ$	
n	CO_2	N_2O	CO_2	N_2O	CO_2	N_2O	CO_2	N_2O	CO_2	N_2O	CO_2	N_2O
1	6.5 ± 0.2 (6.26) (*0.13*)	11.7 ± 0.2 (9.86) (*0.44*)	17 ± 2 (17.5)	23 ± 2 (32.5)	4.8 ± 0.2 (3.75) (*0.14*)	5.5 ± 0.2 (4.08) (*0.20*)	20 ± 2 (21.6)	19 ± 2 (21.7)	3.9 ± 0.2 (3.11) (*0.15*)	5.3 ± 0.2 (3.39) (*0.22*)	16 ± 2 (24.0)	22 ± 2 (25.7)
2	4.9 ± 2 (5.31)	5.6 ± 0.2 (4.22)	15 ± 2 (20.0)	18 ± 2 (22.8)	4.5 ± 0.2 (3.55)	5.4 ± 0.2 (3.85)	20 ± 2 (21.8)	21 ± 2 (21.4)	3.8 ± 0.3 (2.96)	5.2 ± 0.2 (3.10)	17 ± 3 (21.8)	23 ± 2 (22.2)
3	3.9 ± 2	4.6 ± 0.2	12 ± 2	14 ± 2	4.4 ± 0.3	4.5 ± 0.2	22 ± 3	21 ± 2		4.9 ± 0.3		29 ± 3
4	3.7 ± 0.3	4.1 ± 0.5	26 ± 3	19 ± 5		3.9 ± 0.2		21 ± 2				
5		~ 4.0		~ 20								

[a] ΔH° is in kcal/mol and ΔS° is in cal/mol K (standard state, 1 atm). The experimental errors for ΔH° and ΔS° were determined by the method of least squares for the van't Hoff plots. For $n = 1$ and 2, the calculated binding energies (B3LYP/y-311+G(2d,p)), electronic energies, and RHF/6-31G* vibrational energies and entropy changes are shown in parentheses. In $n = 1$, the underlined numbers in parentheses stand for correction energies of the basis set superposition error (BSSE) in kcal/mol. The BSSE corrected binding energy is, for instance, 6.26−0.13 kcal/mol for $C_2H_5^+(CO_2)_1$.

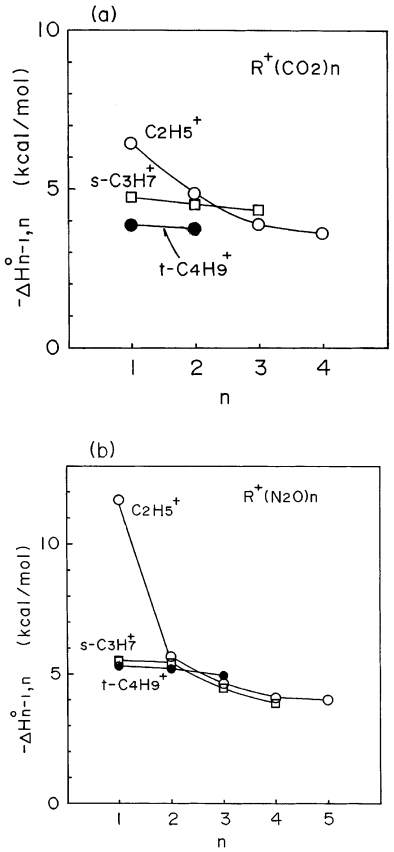

Figure 4. Plots of $-\Delta H_{n-1,n}^\circ$ vs n for clustering reactions $R^+(Sol)_{n-1} + Sol = R^+(Sol)_n$. $R^+ = C_2H_5^+$, s-$C_3H_7^+$, and t-$C_4H_9^+$.

1 with $n = 1$ correspond to those for reaction 7 but not to those for reaction 8.

$$C_2H_5^+(a) + Sol = C_2H_5^+(b)(Sol)_1 \quad (7)$$

$$C_2H_5^+(b) + Sol = C_2H_5^+(b)(Sol)_1 \quad (8)$$

Figure 5 displays the temporal profiles of ions observed after the electron pulse in 2.44 Torr CH_4 containing 6.03 mTorr N_2O at 205.7 K. The N_2OH^+ ($m/z = 45$) is converted to $N_2OH^+(N_2O)_1^+$ ($m/z = 89$) in ~0.1 ms after the electron pulse. In contrast, $C_2H_5^+$ ($m/z = 29$) decays only very slowly with time. The decrease of $C_2H_5^+$ is completely accounted for by the increase of $C_2H_5^+(N_2O)_1$. This indicates that clustering reaction

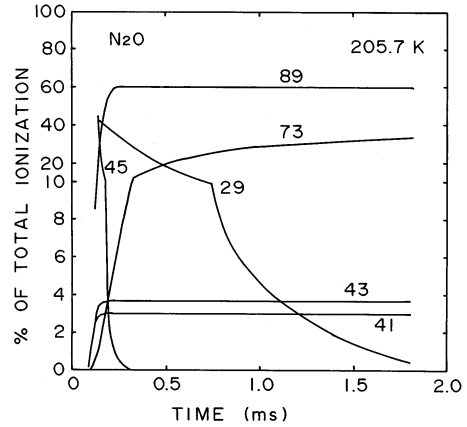

Figure 5. Temporal profiles of ions observed in 2.44 Torr CH_4 and 6.03 mTorr N_2O at 205.7 K. The duration of the 2 keV electron pulse is 30 μs. The observed ions are $C_2H_5^+$ ($m/z = 29$), $C_3H_5^+$ ($m/z = 41$), s-$C_3H_7^+$ ($m/z = 43$), N_2OH^+ ($m/z = 45$), $C_2H_5^+(N_2O)_1$ ($m/z = 73$), and $H^+(N_2O)_2$ ($m/z = 89$).

$C_2H_5^+ + N_2O + M = C_2H_5^+(N_2O)_1 + M$ (reaction with $n = 1$ for Sol = N_2O; M, third body) is unusually slow under the present experimental conditions. The N_2O pressure dependence of the rate constants for the reaction $C_2H_5^+ + N_2O = C_2H_5^+(N_2O)_1$ at 205.0 K was examined. The rate constants are independent of the pressure in Figure S1 of the Supporting Information. This indicates that the reaction is first-order on the N_2O pressure. The temperature dependence of the rate constants of the reaction was plotted as log k vs log T measured in the temperature range of $T = 165-237$ K. The rate constants increase steeply with decrease of temperature in Figure S2 of the Supporting Information. The rate constant k for the reaction is found to be proportional to T^{-10} in the temperature range of 165−204 K.

$$k \propto T^{-10} \ (T = 165-204 \text{ K}) \quad (9)$$

The observed large negative temperature dependence of the rate constant for reaction $C_2H_5^+ + N_2O + M = C_2H_5^+(N_2O)_1 + M$ indicates that the initially formed intermediate complex $C_2H_5^+ \cdot\cdot N_2O$ is short-lived at higher temperatures and its lifetime gets increasingly longer with decrease of temperature as in the case of Sol = CO_2.

The results for the experimentally measured equilibrium constants for reaction 1 (Sol = N_2O) with $n = 1-6$ are displayed as van't Hoff plots in Figure 1b. The enthalpy and entropy changes obtained from Figure 1b are summarized in Table 1.

A large gap in the van't Hoff plots between $n = 1$ and 2 suggests the covalent character in the bond $C_2H_5^+\cdots N_2O$. It is reasonable to assume that the observed clustering reaction 1 ($n = 1$ for N_2O) corresponds to reaction 7 rather than reaction 8. It is not clear to what extent the cluster ions $C_2H_5^+(b)(N_2O)_n$ are contaminated by $C_2H_5^+(a)(N_2O)_n$. Judging from the straight van't Hoff plots in Figure 1b and the N_2O pressure-independent equilibrium constants for reaction 1 (Figure 3b) with $n = 1-3$, the contamination by $C_2H_5^+(a)(N_2O)_n$ may be negligible with $n = 1-3$.

The equilibria for clustering reaction 1 of Sol = N_2O with $n = 2$ and 3 were found to be established almost right after the electron pulse. However, the equilibrium constants with $n = 4$ and 5 in Figure 1b deviate from the straight lines in the higher temperature region. This suggests the presence of $C_2H_5^+(a)(N_2O)_n$ as well as $C_2H_5^+(b)(N_2O)_n$ with $n = 4$ or 5 as in the case of Sol = CO_2. With a decrease of temperature, the rate of the isomerization reaction $a \rightarrow b$ decreases due to the lack of thermal energy. The van't Hoff plots with $n = 5$ are too erratic to obtain the reliable thermochemical value.

Figure 3b represents the N_2O pressure dependence on the measured equilibrium constants for reaction 1 with $n = 2-5$. The equilibrium constants with $n = 2$ at 145.8 K, $n = 3$ at 132.6 K, and $n = 4$ at 116.5 K are independent of the N_2O pressure. In these cases, the equilibrium constants lie on the straight van't Hoff plots (Figure 1b). In contrast, those with $n = 4$ at 132.6 K and $n = 5$ at 113.4 K decrease and approach asymptotically the equilibrium values with increase of the partial pressure of N_2O. This trend is similar to the case of Sol = CO_2, i.e., the isomerization reaction $a \rightarrow b$ is enhanced by the interaction of the less stable complex $[(C_2H_5(a)(N_2O)]^+$ with the N_2O molecule.

In Figure 4b is shown the n dependence of the values of $-\Delta H_{n-1,n}^\circ$ for reaction 1 for Sol = N_2O. The sudden decrease of $-\Delta H_{n-1,n}^\circ$ with $n = 1 \rightarrow 2$ clearly indicates the formation of the incipient covalent bond in the cluster $C_2H_5^+(N_2O)$. The enthalpy change ($-\Delta H_{0,1}^\circ = 11.7 \pm .2$ kcal/mol) is almost two times as large as that for s-$C_3H_7^+(N_2O)_{0\rightarrow1}$ (5.5 ± 0.2 kcal/mol) (see Table 1). This clearly indicates that $C_2H_5^+$ is a stronger electrophilic reagent than s-$C_3H_7^+$. The larger $-\Delta H_{0,1}^\circ$ for N_2O than that for CO_2 ($6.5 \pm .2$ kcal/mol) is reminiscent of the fact that the ions NO^+, O_2^+, and H_3O^+ form stronger bonds with N_2O than CO_2.[12] It is apparent that N_2O is a much stronger nucleophilic reagent than the isoelectronic CO_2. Because the nonclassical $C_2H_5^+(a)$ isomerizes to the classical $C_2H_5^+(b)$ in the clustering reactions, the thermochemical stabilities of the clusters $C_2H_5^+(a)(Sol)_n$ could not be determined.

3.2. Clustering Reaction of s-$C_3H_7^+$ and t-$C_4H_9^+$ with Sol. Figures 6 and 7 display the van't Hoff plots for clustering reactions 2 and 3, respectively, for Sol = CO_2 and N_2O. The obtained thermochemical values are summarized in Table 1. The $-\Delta H_{n-1,n}^\circ$ values with n are shown in Figure 4. The relatively small values of $-\Delta H_{n-1,n}^\circ$ for those reactions indicate that the nature of the bonding in the clusters s-$C_3H_7^+(Sol)_n$ and t-$C_4H_9^+(Sol)_n$ are mainly electrostatic.

4. Calculated Results and Discussion

Geometries of three carbonium ions were calculated first (Figure S3 in the Supporting Information). A striking result is that ethyl cation stays only in the bridge form (a). The bridge form (a) of $C_2H_5^+$ lies in a single energy minimum. This result by B3LYP/6-311+G(2d,p) calculations is in contrast with previous ones,[5-9] which suggested or indicated the double energy minima (two geometric isomers) for $C_2H_5^+$. That result

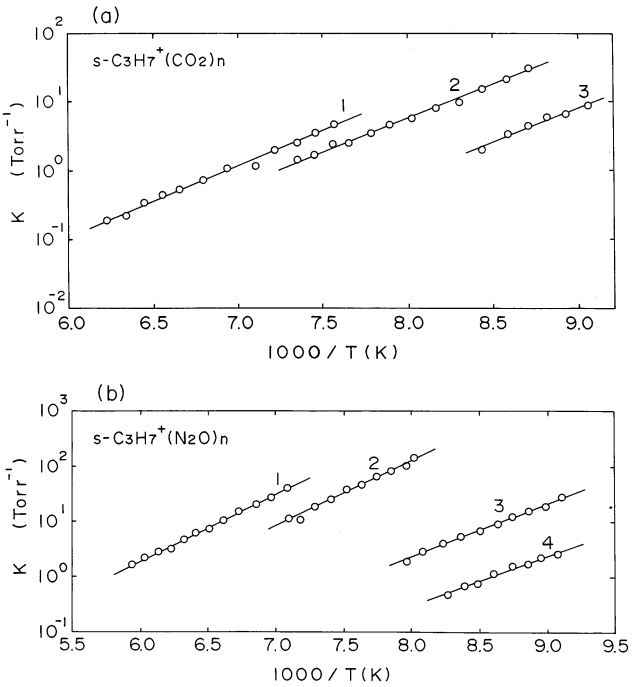

Figure 6. van't Hoff plots for equilibria of clustering reaction, s-$C_3H_7^+(Sol)_{n-1}$ + Sol = s-$C_3H_7^+(Sol)_n$.

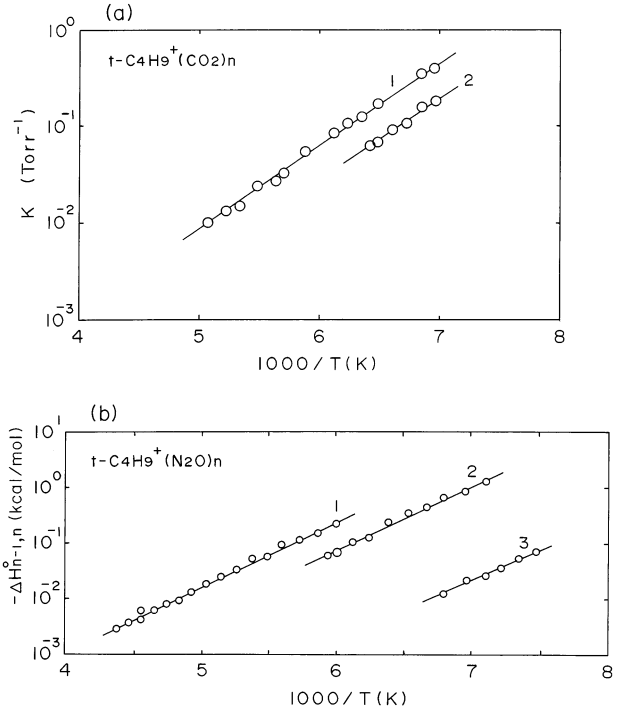

Figure 7. van't Hoff plots for equilibria of clustering reaction, t-$C_4H_9^+(Sol)_{n-1}$ + Sol = t-$C_4H_9^+(Sol)_n$.

(the single minimum a) is confirmed by higher level calculations, B3LYP/6-311+G(3df,2p), MP4(SDQ)/6-311G(d,p), and QCISD(T)/6-311G(d,p). For the energy change with respect to the variation, there is a slight shoulder at $\angle H-C-C \approx 95°$, which corresponds to the classical structure. The source for the bridged structure is illustrated in Scheme 2.

Let us consider $C_2H_5^+$ as an ethylene molecule plus a hydrogen atom minus an electron. The ionization potential of H• (13.6 eV) is much larger than that of C_2H_4 (10.5 eV). Then, the ethyl cation is regarded as an interacting system not between proton and ethylene but between hydrogen atom and ethylene

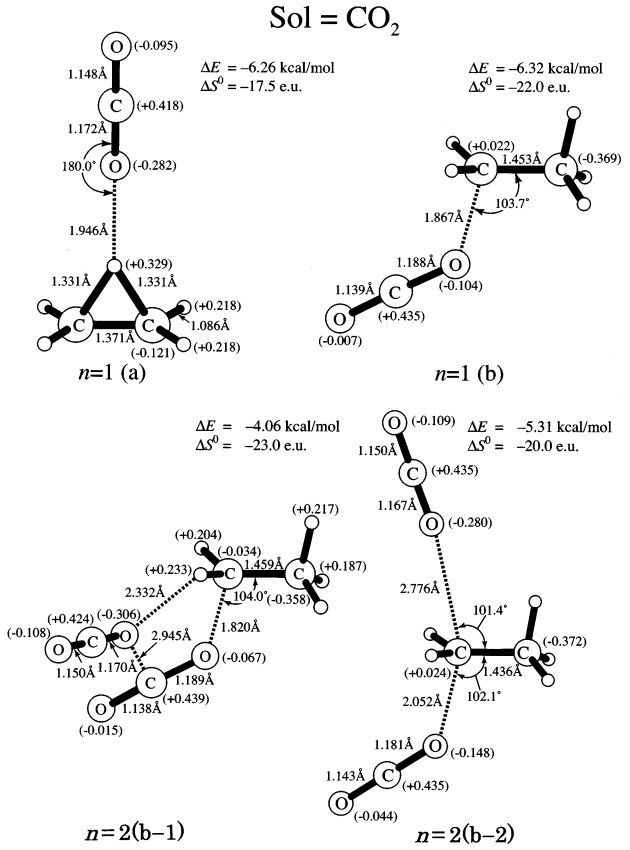

Figure 8. Geometries of $C_2H_5^+(CO_2)_n$. The calculated energies and entropy changes are also shown.

SCHEME 2: Origin of the Nonclassical Ethyl Cation

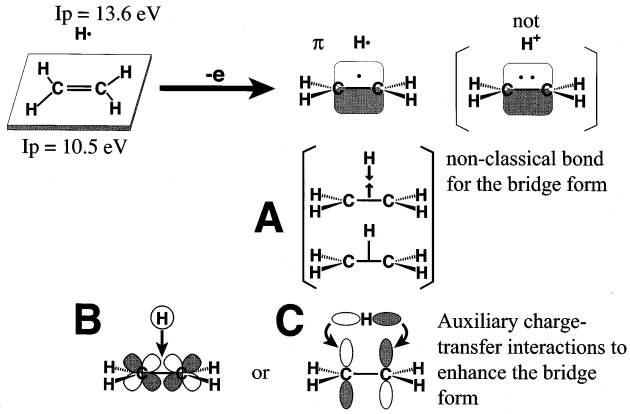

cation radical. Because the odd electron belongs to the nodeless π orbital, the spin density is maximum at the middle of C−C bond. The singlet interaction gives panel A in Scheme 2.[17]

In geometries of propyl and butyl cations, single C−C covalent bonds (1.43 Å of *s*-$C_3H_7^+$ and 1.46 Å of *t*-$C_4H_9^+$) are shorter than that (1.54 Å) of ethane due to hyperconjugation (Figure S3 in the Supporting Information). Figure 8 shows geometries of $C_2H_5^+(CO_2)_n$ complexes. As predicted in Section 3.1, there are two geometric isomers, $n = 1(a)$ and $n = 1(b)$. Prior to calculations, hydrogen bond complexes of $H_2C(H)CH-H\cdots O{=}C{=}O$ were expected. However, this initial geometry is converted to that in $n = 1(a)$. In $n = 1(a)$, the nonclassical bridge form of $C_2H_5^+$ is retained and the shift of the electronic charge, $O{=}C{=}O \rightarrow C_2H_5^+$ is small (0.041). In the isomer $n = 1(b)$, $C_2H_5^+$ becomes a classical geometry where the methylene cation center is coordinated to OCO. The charge shift is 0.324,

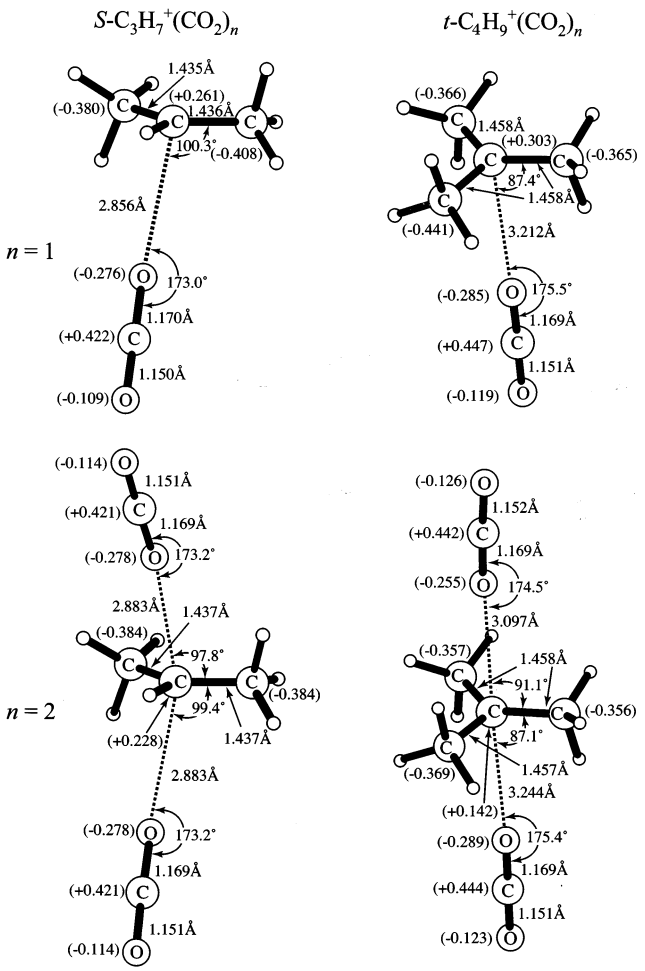

Figure 9. Geometries and changes of energy and entropy of *s*-$C_3H_7^+(CO_2)_n$ and *t*-$C_4H_9^+(CO_2)_n$.

and the charge transfer makes $C_2H_5^+$ the classical form. Two isomers have almost the same energetic stability (−6.26 and −6.32 kcal/mol in Figure 8). The energy difference may be overcome by $-T \times \Delta S$ in Gibbs free energies, because $n = 1(a)$ is entropically more favorable than $n = 1(b)$. For $n = 2$, also, geometric isomers were obtained.[18] In $n = 2(b-1)$, the second CO_2 molecule is linked both with the first CO_2 and the ethylenic hydrogen atom. The $n = 2(b-2)$ has an expected sandwich form where the second C···O distance (2.776 Å) is much larger than the first one (2.052 Å). This difference indicates that the cation center of $C_2H_5^+$ is neutralized substantially by the first CO_2 coordination. The primary carbonium ion cannot undergo the equivalent CO_2 sandwich coordination. The isomer $n = 2(b-2)$ is more stable than $n = 2(b-1)$ energetically and entropically. Figure 8 has demonstrated that the entropically favorable $n = 1(a)$ cluster retains the bridge $C_2H_5^+$ form and the $n = 2$ one has the classical form. The mobility of the central hydrogen arises from the nonclassical bond in the nodeless π orbital (Scheme 2).

Figure 9 shows geometries of *s*-$C_3H_7^+(CO_2)_n$ and *t*-$C_4H_9^+(CO_2)_n$. As compared with the C···O distance, 1.867 Å of $n = 1(b)$ (Figure 8), those in $n = 1$ are very large, 2.856 and 3.212 Å. Accordingly, the charge shifts (0.037 for OCO → *s*-$C_3H_7^+$ and 0.043 for OCO → *t*-$C_4H_9^+$) are much smaller than that (0.324 for OCO → $C_2H_5^+(b)$ in Figure 8). The weak interaction is also shown by the almost linear coordination, $C^+\cdots O{=}C{=}O$. For $n = 2$, almost equivalent sandwich coordinations have been obtained. Noteworthy is that the C···O distances are nearly

the same for $n = 1$ and 2 of $t\text{-}C_4H_9^+(CO_2)_n$. The invariance corresponds to the similar value of $\Delta H_{0,1}^\circ = -3.9$ kcal/mol and $\Delta H_{1,2}^\circ = -3.8$ kcal/mol in Table 1.[19]

The *tert*-butyl cation is almost free from the base coordination regardless of the base strength. Hyperconjugation by three methyl groups makes nearly the central carbon an inert atom.

5. Concluding Remarks

In this work, gas phase clustering reactions of three carbonium ions with weak and strong bases (CO_2 and N_2O) have been studied. The ethyl cation has been found to be of a nonclassical bridge form as a sole energy minimum. The physical picture of the nonclassical $C_2H_5^+$ form has been proposed (Scheme 2). The base coordination turns it out to a classical form. Because contributions of geometric isomers to the change of Gibbs free energy are competitive in the temperature range measured, the scattered van't Hoff plots have been obtained. Stability of carbonium ions against nucleophiles is examined explicitly in the present gas phase experiment. The primary carbonium ion, ethyl cation, is quite sensitive to nucleophilicity of bases. In contrast, the tertiary ion is not susceptible to it. The solvation strength of $s\text{-}C_3H_7^+$ is close not to that of $C_2H_5^+$ but to that of $t\text{-}C_4H_9^+$. In Table 1, the calculated $\Delta H_{n-1,n}^\circ$ and $\Delta S_{n-1,n}^\circ$ values are in fair agreement with the observed ones.

Supporting Information Available: N_2O pressure dependence on the rate constants for reaction $C_2H_5^+ + N_2O + CH_4 = C_2H_5^+(N_2O)_1 + CH_4$ in Figure S1; relation between the ion source temperature and the rate constants for the reaction in Figure S2; geometries and electronic charges of $C_2H_5^+$, $s\text{-}C_3H_7^+$, and $t\text{-}C_4H_9^+$ in Figure S3; those of $C_2H_5^+(N_2O)_n$ in Figure S4; and those of $s\text{-}C_3H_7^+(N_2O)_n$ and $t\text{-}C_4H_9^+(N_2O)_n$. This material is available free of charge via the Internet at http://pubs.acs.org.

References and Notes

(1) Kebarle, P. *Ann. Rev. Phys. Chem.* **1977**, *28*, 445.
(2) Hiraoka, K.; Kebarle, P. *J. Chem. Phys.* **1975**, *62*, 2267.
(3) Hiraoka, K.; Kebarle, P. *J. Am. Chem. Soc.* **1975**, *97*, 4179.
(4) Hoffmann, R. *J. Chem. Phys.* **1973**, *40*, 2480.
(5) Koeler, H.-J.; Lischka, H. *Chem. Phys. Lett*. **1978**, *58*, 175.
(6) Ausloos, P.; Rebbert, R. E.; Sieck, L. W.; Tiernan, T. O. *J. Am. Chem. Soc.* **1972**, *94*, 8939.
(7) Houle, F. A., Beauchamp, J. L. *J. Am. Chem. Soc.* **1979**, *101*, 4067.
(8) Gellene, G. I.; Kleinrock, N. S.; Porter, R. F. *J. Chem. Phys.* **1983**, *78*, 1795.
(9) Hirao, K.; Yamabe, S. *Chem. Phys.* **1984**, *89*, 237.
(10) Hiraoka, K.; Kebarle, P. *J. Am. Chem. Soc.* **1976**, *98*, 6119.
(11) Yeh, L. I.; Price, J. M.; Lee, Y. T. *J. Am. Chem. Soc.* **1989**, *111*, 5597.
(12) Hiraoka, K.; Fujimaki, S.; Aruga, K.; Sato, T.; Yamabe, S. *J. Phys. Chem.* **1994**, *101*, 4073.
(13) Hiraoka, K. *J. Chem. Phys.* **1987**, *87*, 4048.
(14) Becke, A. D. *J. Chem. Phys.* **1993**, *98*, 5648.
(15) Frisch, M. J.; Trucks, G. W.; Schlegel, H. B.; Gill, P. M. W.; Johnson, B. G.; Robb, M. A.; Cheeseman, J. R.; Keith, T.; Petersson, G. A.; Montgomery, J. A.; Raghavachari, K.; Al-Laham, M. A.; Zakrzewski, V. G.; Ortiz, J. V.; Foresman, J. B.; Cioslowski, J.; Stefanov, B. B.; Nanayakkara, A.; Challacombe, M.; Peng, C. Y.; Ayala, P. Y.; Chen, W.; Wong, M. W.; Andres, J. L.; Replogle, E. S.; Gomperts, R.; Martin, R. L.; Fox, D. J.; Binkley, J. S.; Defrees, D. J.; Baker, J.; Stewart, J. P.; Head-Gordon, M.; Gonzalez, C.; Pople, J. A. *Gaussian 94*, revision A.1; Gaussian, Inc.: Pittsburgh, PA, 1995.
(16) Hiraoka, K.; Mori, T.; Yamabe, S. *Chem. Phys. Lett*. **1993**, *207*, 178.
(17) This nonclassical "covalent bond" cannot be shown by Hartree−Fock wave functions with small basis sets. Correlated wave functions such as CI, MCSCF, and Moeller−Plesset (MP) and density functional theory calculations can show the nonclassic picture. There are two factors for promoting this picture even with Hartree−Fock wave functions. One is inclusion of d type polarization functions to carbon atoms. The systematic combination of d orbitals (panel B in Scheme 2) may give a central location of the hydrogen atom. The other is inclusion of p orbitals onto the hydrogen atom (panel C in Scheme 2), which allows the back p_π charge transfer for fixing the position of hydrogen atom. Thus, the extension of basis sets enhances the stability of $C_2H_5^+(a)$.
(18) The third and the least stable isomer $n = 2(a)$ was also obtained, where the $n = 1(a)$ moiety and a CO_2 molecule bound in the ethylenic plane are included. $n = 2(a)$ is 1.52 kcal/mol less stable than $n = 2(b-2)$ ($C_2H_5^+(CO_2)_n$ in Figure 8). For the corresponding $C_2H_5^+(N_2O)_n$, $n = 2(a)$ is 6.7 kcal/mol less stable than $n = 2(b-1)$ in Figure S4. The $n = 2(a)$ geometry of $C_2H_5^+(CO_2)_2$ is extremely floppy and is variable by computational methods. For instance, B3LYP/6-311+G(2d,p) gives the $n = 2(a-1)$ geometry, while RHF/(6-31)G* gives the $n = 2(a-2)$ one. Their lowest frequencies of $n = 2(a-1)$ and $n = 2(a-2)$ are 10.7 and 7.7 cm^{-1}, respectively, which shows that the $n = 2$ geometry is not so meaningful.

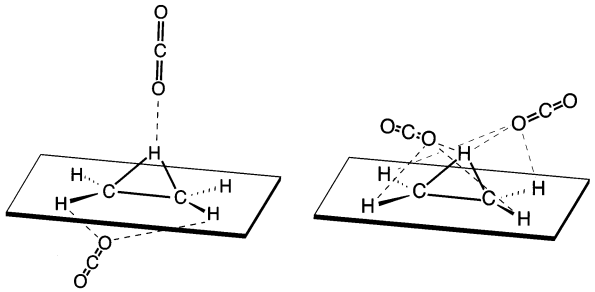

(19) Figure S4 in the Supporting Information exhibits geometries of $C_2H_5^+(N_2O)_n$. As those in Figure 8, there are geometric isomers for $n = 1$ and 2. As expected by the larger nucleophilicity of N_2O than that of CO_2,[12] H···O (1.911 Å, $n = 1(a)$) and O···C (1.688 Å, $n = 1(b)$) distances in $C_2H_5^+(N_2O)_1$ are shorter than the corresponding ones in $C_2H_5^+(CO_2)_1$. In $n = 2(b-2)$, the first C···O distance is 1.715 Å and the second one is 2.922 Å. Because the first N_2O is linked strongly, the second one is far away from the cation center. This trend is larger than that in Figure 8, and the base coordination geometry depends on its strength. The ΔE difference between $n = 2(b-1)$ and $n = 2(b-2)$ is very small, and in free energies, their relative stabilities are completely temperature-dependent. Figure S5 shows geometries of $s\text{-}C_3H_7^+(N_2O)_n$ and $t\text{-}C_4H_9^+(N_2O)_n$, which correspond to those of CO_2 coordinations in Figure 9. Despite the difference of nucleophilicity between CO_2 and N_2O, the intermolecular distances are similar, ~2.8 Å for $s\text{-}C_3H_7^+$ and ~3.2 Å for $t\text{-}C_4H_9^+$. The strong basicity of N_2O is reflected only in the C···O−N angles (163−164°) of $s\text{-}C_3H_7^+(N_2O)_n$, which indicates the slight coordination directionality. However, those angles are all the same (~175°) in $t\text{-}C_4H_9^+(N_2O)_n$.